GRISPE

Guidelines and **R**ecommendations for **I**ntegrating **S**pecific **P**rofiled steel sheets in the **E**urocodes (**GRISPE**)

WP4 Doc 1 Version 01

Background document

Working Package 4

Deliverable D 4.1

Guidelines and Recommandations for Integrating Specific Profiled Steels sheets in the Eurocodes (GRISPE)

Project co-funded under the Research Fund for Coal and Steel
Grant agreement No RFCS-CT-2013-00018
Proposal No RFS-PR-12027

Author(s)	
M. BLANC, BACACIER	
T. RENAUX, Société Bretonne de Profilage – Groupe JORIS IDE	
Drafting history	
Draft Version 1 (part 1)	*24th October 2013*
Draft Version 1 (part 2)	*31st October 2013*
Final Version	*30th November 2013*

Dissemination Level		
PU	*Public*	
PP	*Restricted to the Commission Services, the Coal and Steel Technical Groups and the European Committee for Standardisation (CEN)*	
RE	*Restricted to a group specified by the Beneficiaries*	
CO	*Confidential, only for Beneficiaries (including the Commission services)*	***X***

Verification and Approval
Coordinator
WP4 Leader
Other Beneficiaries

Deliverable	
D 4.1 Background document : synthesis of the state of art	***Due date : 30th Nov. 13*** ***Completion date:30th Nov. 13***

Summary

1. Context of WP 4

In the story of steel building envelope, claddings planks and cassettes were developed for esthetical applications. Unlike the corrugated steel sheets for "traditional" cladding, consideration of aesthetics has taken over the mechanical aspect.
Indeed, research of performance compared to wind load resistance has been replaced by the research of hidden fixings solutions as below:

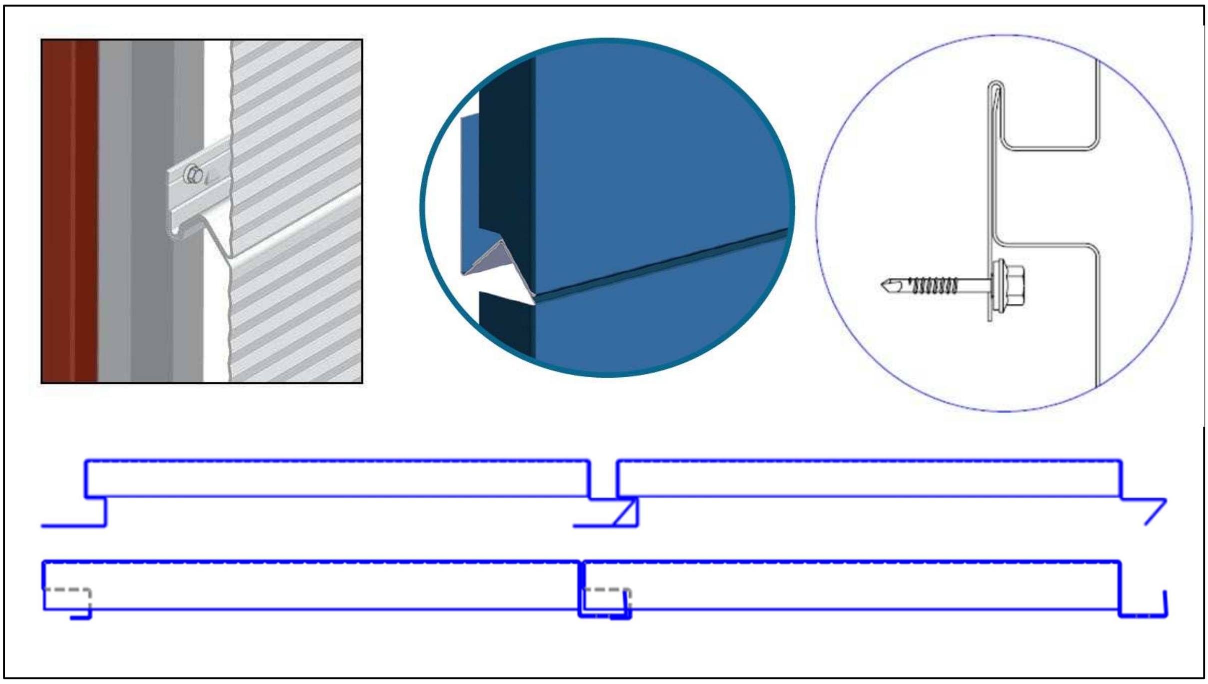

Figure 1: Examples of hidden fixing (non-limiting)

1.1. Actual European standards developed for steel sheets

Design of "classic" profiles for cladding uses two types of methods:

- By calculation
- And/or by tests

In Europe, before the arrival of the Eurocodes, the choice of one or two methods operated at national level. While in Germany the standards authorized the use of the calculations [1] and the experimental [2], the France retains only the method by testing [3].
The introduction of the Eurocodes provides a common method of design that allows the use of tests and/or analytical formulas [4] [5], but claddings planks are not covered by the scope (Figure 2 and Figure 3).

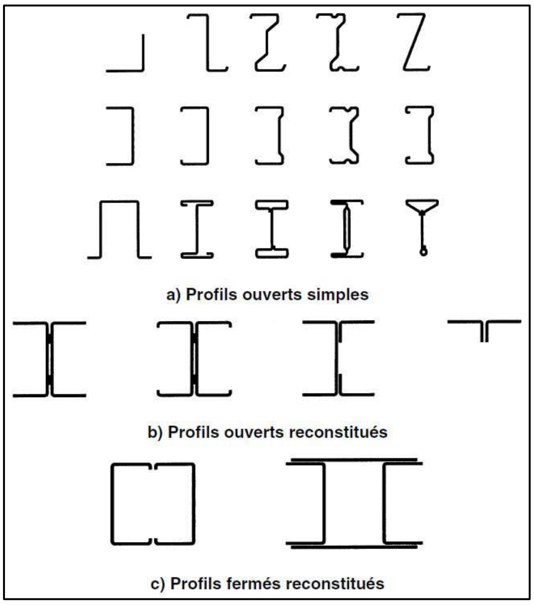

Figure 2: Common geometries of steel members

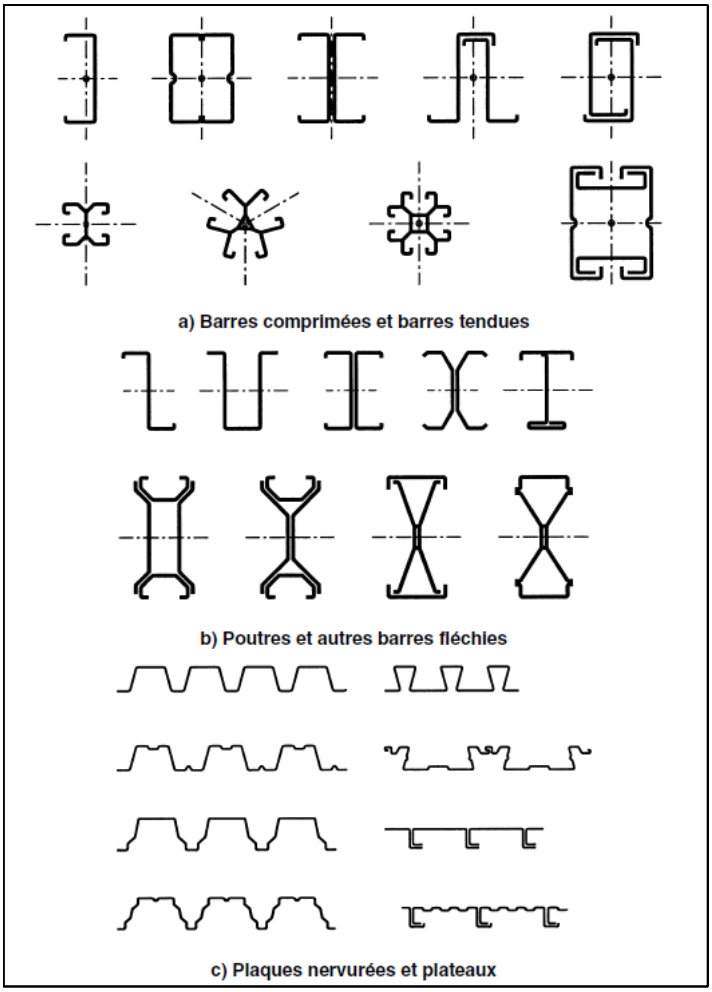

Figure 3: Examples of corrugated steel sheets and profiles

1.2. Actual methods used for designing

To overcome this situation, different strategies have been implemented.
At European level, cladding planks and cassettes can be designed across a European Technical Approval according the ETAG 34 part 1 and 2 [6] [7]. The wind load behaviour is determined by tests like method chosen in France [8] or across a French Technical Assessment (AT/DTA). But although these methods are loyal to the real assembly with a specific distance between supports, they don't allow interpolation or extrapolation to other spans. Moreover, this kind of test present a high cost and it's not possible to view and analyse the behaviour of the hidden joint on support and in span for cladding plank with hidden fixing.
For cladding cassettes, some manufacturers try with success to consider certain parts of Eurocode [9] but in situation of hidden fixings, this method is not applicable.

1.2.1. Designing by tests

Actual experimental method in France [3] adapted to cladding planks and cassettes helps to have accurate information about physical phenomena.
Apply and determine resistance under wind pressure drive to situation below (Figure 4 c)):

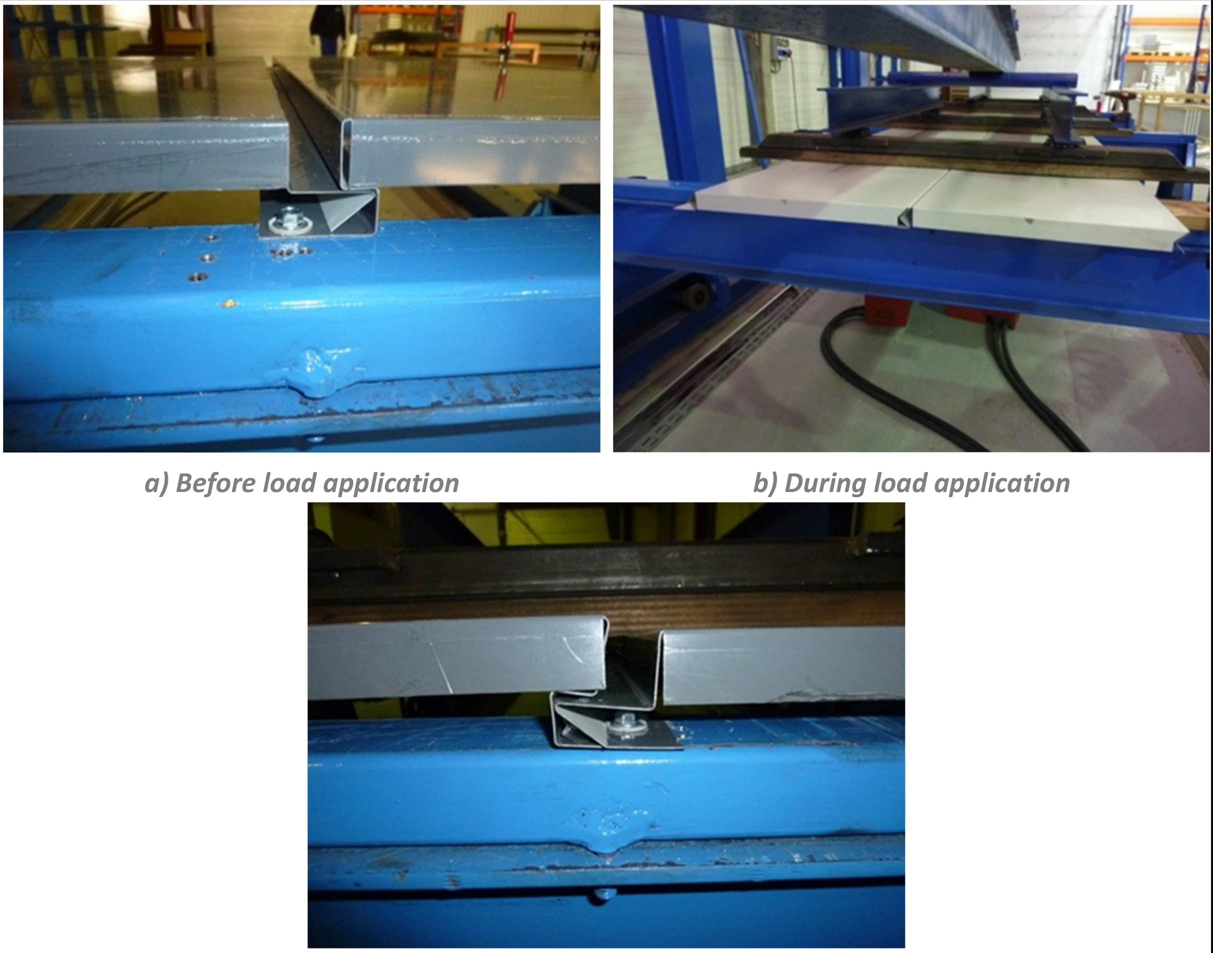

a) Before load application

b) During load application

c) End of the test

Figure 4: Wind pressure test with linear loads

Under wind depression loads, the behaviour and rupture is function of the technology of the hidden joint. In the situation of Figure 5, no rupture is found but in fact a progressive dislocation. In the situation of Figure 6, the dislocation is brutal.

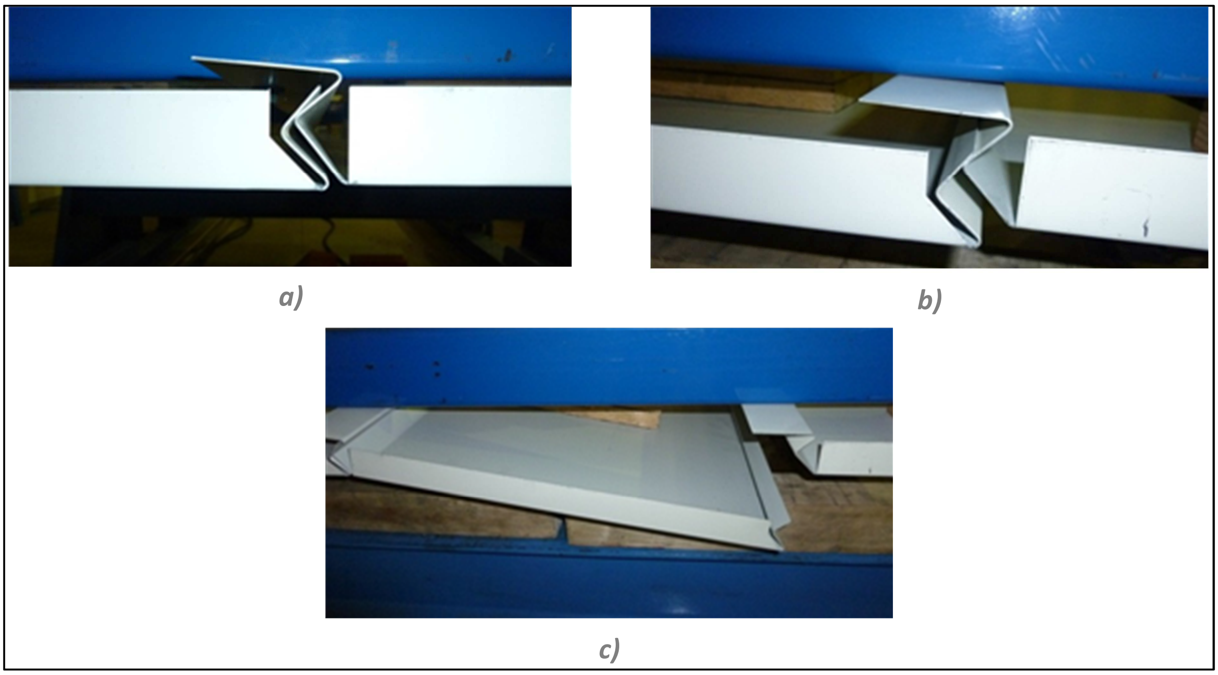

Figure 5: Cladding planks dislocation during wind suction tests

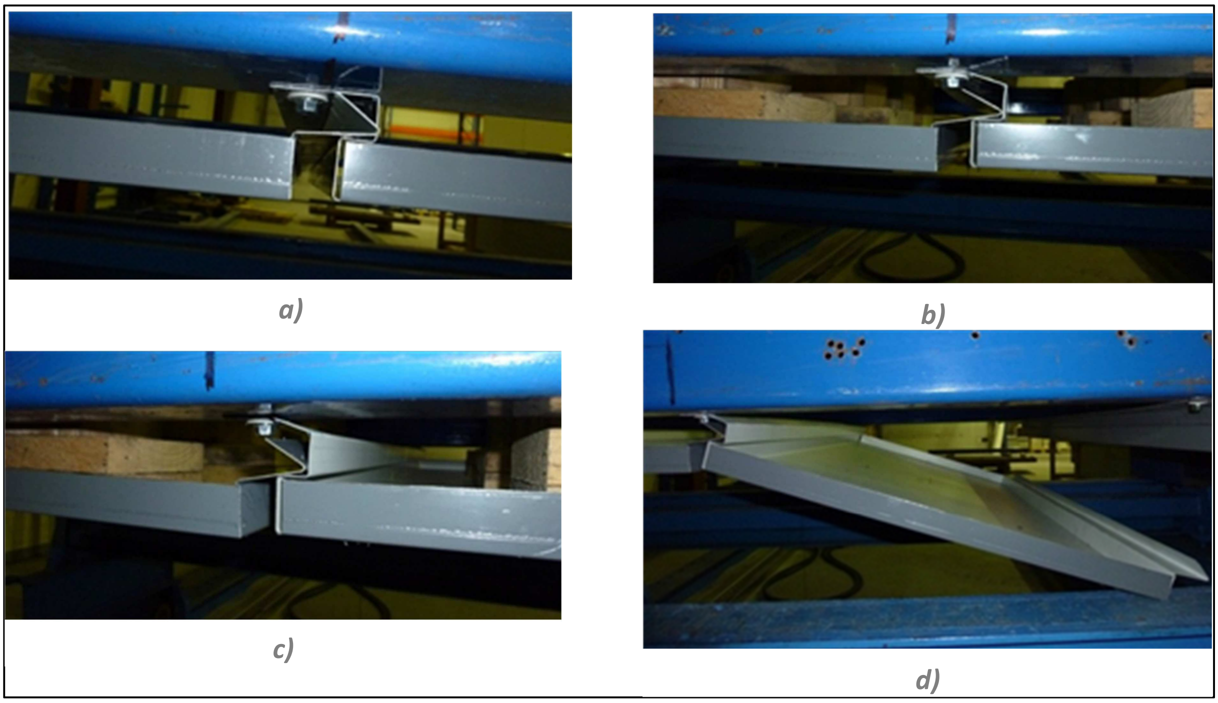

Figure 6: Cladding cassettes dislocation during wind suction tests

1.2.2. Designing by calculation [4] [5]

The closest form of section, for interlocking planks and cassettes, for which a design method is given in Eurocode EN 1993-1-3, is liner tray. In bending, this method should give good results.

The principle of this method is to consider that the wide flange (without stiffeners in our case) is not fully effective in bending, whether it is tensed or compressed. The section is then calculated as a beam considering this effective flange instead of the full wide one. The estimation of this effective part of the wide flange depends on the stress:

- In compression: both shear lag and plate buckling effects according to EN 1993-1-5 must be considered. These effects are evaluated with the wide flange simplified to a plate without any stiffeners.
- In tension: the possible flange curling is taken into account, considering the cross inertia of the flange due to the stiffeners. In our case, the wide flange is a plate. So we should determine the effective part of this only using shear lag effect according to EN 1993-1-5.

1.2.2.1. Behaviour of the wide flange

Shear lag effect

In our case, the effective width of the wide flange $b_{u,eff}$ for shear lag is determined from:

$$b_{u,eff} = \beta \cdot b_0$$

where:

- β: effective[s] factor of the flange;
- b_0: reference width of the flange.

In our case, it is to say for an internal flange, and the gross overall width b_u:

$$b_0 = \frac{b_u}{2}$$

The effective factor β for shear lag depends on the location of the studied cross section. Its determination relies on the slenderness of the flange which is linked to the effective length of the span. The values of effective lengths for different configurations of span are given below:

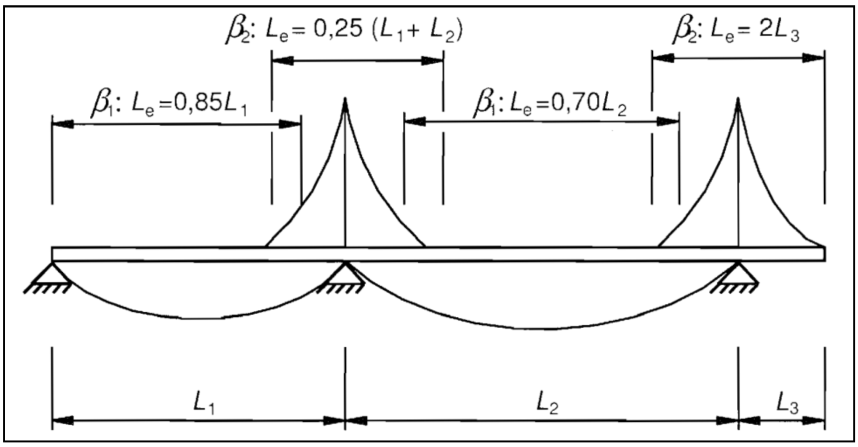

Figure 7: Effectives lengths for shear lag

As the wide flange is a plate without stiffeners, its slenderness κ is:

$$\kappa = \frac{b_0}{L_e}$$

The effective factor β is given in the table below:

κ	Verification	β – value
$\kappa \leq 0{,}02$		$\beta = 1{,}0$
$0{,}02 < \kappa \leq 0{,}70$	sagging bending	$\beta = \beta_1 = \dfrac{1}{1 + 6{,}4\,\kappa^2}$
	hogging bending	$\beta = \beta_2 = \dfrac{1}{1 + 6{,}0\left(\kappa - \dfrac{1}{2500\,\kappa}\right) + 1{,}6\,\kappa^2}$
$> 0{,}70$	sagging bending	$\beta = \beta_1 = \dfrac{1}{5{,}9\,\kappa}$
	hogging bending	$\beta = \beta_2 = \dfrac{1}{8{,}6\,\kappa}$
all κ	end support	$\beta_0 = (0{,}55 + 0{,}025 / \kappa)\,\beta_1$, but $\beta_0 < \beta_1$
all κ	Cantilever	$\beta = \beta_2$ at support and at the end

Figure 8: Values of effective factor β

This effect is to be considered for the wide flange whether it is in tension or in compression

Plate buckling effect on the wide flange

The effective area of the wide flange for the effects of plate buckling $A_{c,eff}$ is given below:

$$A_{c,eff} = \rho \cdot A_c$$

where:

- ρ: effective$^{\rho}$ factor of the flange;
- A_c: area of the gross cross-sectional area of the flange (i.e. $b_u \times t$).

As for shear lag, the effective$^{\rho}$ factor ρ depends on the slenderness $\bar{\lambda}_p$ which is:

$$\bar{\lambda}_p = \sqrt{\frac{f_y}{\sigma_{cr}}} = \frac{b_u/t}{28{,}4 \cdot \varepsilon \cdot \sqrt{k_\sigma}}$$

In our case, the wide flange is an internal element fully compressed with a constant stress, i.e. the stress ratio $\psi = 1$ and the corresponding buckling factor is:

$$k_\sigma = 4{,}0$$

In the formula above

$$\varepsilon = \sqrt{\frac{235}{f_y}}$$

f_y is the basic yield strength (N/mm^2)

Stress distribution (compression positive)	Effective[p] width b_{eff}
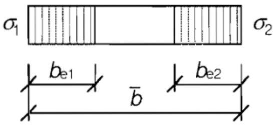	$\underline{\psi = 1}$: $b_{eff} = \rho\ \bar{b}$ $b_{e1} = 0{,}5\ b_{eff}$ $\quad b_{e2} = 0{,}5\ b_{eff}$

Figure 9: Effectives parts of the wide flange

Then, each effective part of the flange, b_{e1} and b_{e2} given above, is associated to the closest web.

1.2.2.2. Buckling effect on the web

As for the wide flange, the effective area of the web $A_{c,eff}$ is given by:

$$A_{c,eff} = \rho \cdot A_c$$

The difference is that the stress ratio ψ is different because the web is part tensed and part compressed.

Stress distribution (compression positive)	Effective[p] width b_{eff}
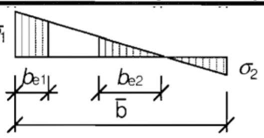	$b_{eff} = \rho\ b_c = \rho\ \bar{b}\ /\ (1-\psi)$ $b_{e1} = 0{,}4\ b_{eff}$ $\quad b_{e2} = 0{,}6\ b_{eff}$

$\psi = \sigma_2/\sigma_1$	1	$1 > \psi > 0$	0	$0 > \psi > -1$	-1	AC1 $-1 > \psi \geq -3$ AC1
Buckling factor k_σ	4,0	$8{,}2\ /\ (1{,}05 + \psi)$	7,81	$7{,}81 - 6{,}29\psi + 9{,}78\psi^2$	23,9	$5{,}98\ (1 - \psi)^2$

Figure 10: Effectives parts of the web

As we can see above, the buckling factor k_σ depends on this stress ratio ψ and so does the slenderness $\bar{\lambda}_p$, i.e. they depend on the position of the centroid of the section.

1.2.2.3. Performances of the section

The moment resistance is determined using a step-by-step procedure. This procedure depends on the stress in the wide flange.

Wide flange in compression

Step 1: Determine the position of the centroid of the section, considering fully effective web and small flange, and the effective part of the wide flange (considering both shear lag and buckling effects)

Step 2: Find the centroid of the effective cross section, considering the effective part of the web calculated with the stress ration ψ deducted from the first centroid, and deduct the moment resistance $M_{c,Rd}$:

$$M_{c,Rd} = 0{,}8 \cdot W_{eff,\min} \cdot \frac{f_{yb}}{\gamma_{M0}}$$

where:

$$W_{eff,\min} = \frac{I_{y,eff}}{\max(z_c; z_t)}$$

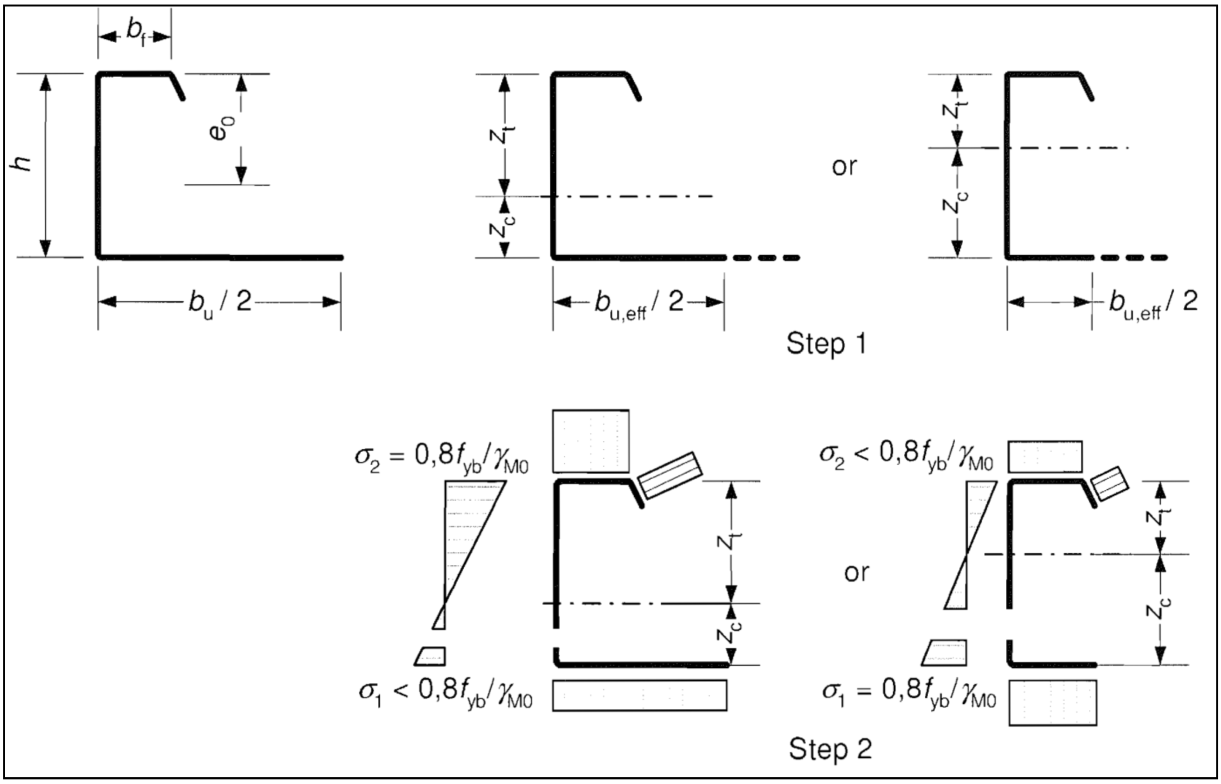

Figure 11: Calculation method for wide flange in compression

Wide flange in tension

Step 1: Determine the position of the centroid of the section, considering a fully effective web and the effective part of the wide flange (considering only shear lag effect)

Step 2: Determine the position of the centroid of the section considering the effective part of the web calculated with the stress ration ψ deducted from the first centroid and the effective part of the wide flange

Step 3: Find the centroid of the effective cross section considering the effective part of the web, of the wide flange and of the small flange, and deduct the moment resistance $M_{c,Rd}$:

$$M_{c,Rd} = 0{,}8 \cdot W_{eff,\min} \cdot \frac{f_{yb}}{\gamma_{M0}}$$

where:

$$W_{eff,\min} = \frac{I_{y,eff}}{\max(z_c; z_t)}$$

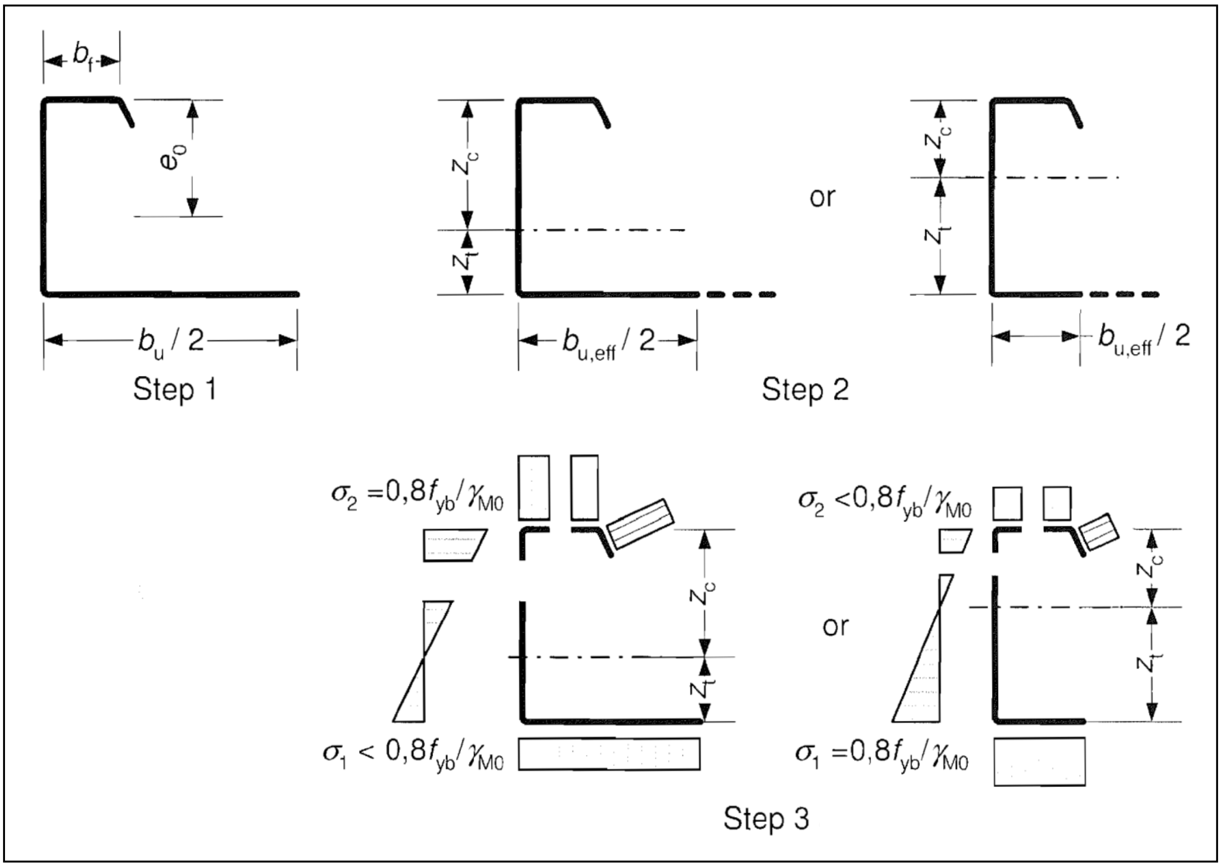

Figure 12: Calculation method for wide flange in tension

1.3. Introducing the second part of the synthesis of state of art

The main difficulty of WP 4 lies in determining suitable test campaigns to identify all conditions and characteristics governing dislocation phenomena that drive the behaviour under depression load of hidden fixed cladding planks and cassettes.
This also means that suitable measures devices must be implemented.
The establishment of analytical formulas characteristics of dislocation phenomena may appeal to parts of Eurocode 3 Part 1-3, paragraph 5 and 10.1 in particular, but also standard prefiguring Eurocodes [1] [10].

2. Critical description of reference [9]

Part of this document deals with the design of a cladding cassette that appeal to the classical theory of plates and certain formulas of EN 1993-1-3 (and correctly to EN 1993-1-5), similar to example below:

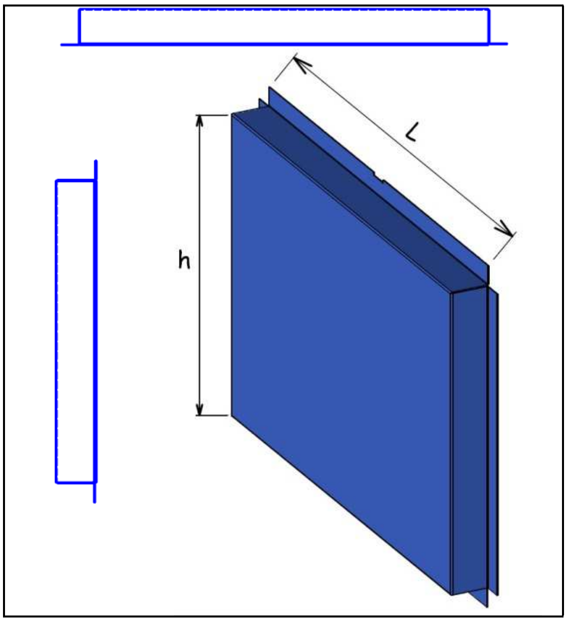

Figure 13: Cladding cassette similar the one studied

2.1.1. Design and background

The design of the cladding cassette needs especially to check the material thickness and the height.

Due to the type of product and its implementation, the cladding cassette is a rectangular simply supported thin plate with rotational springs at all four edges (Fig. 8).

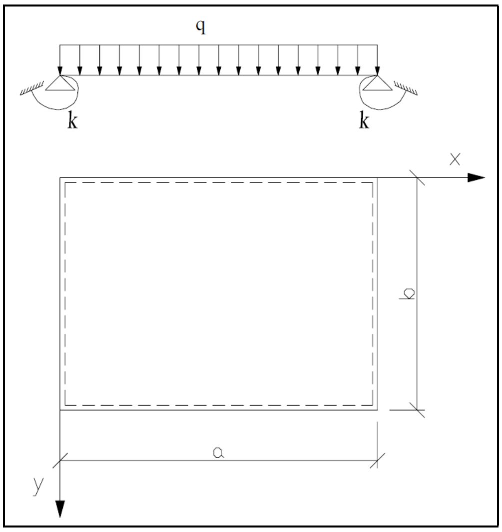

Figure 14: Mechanical model

2.1.2. Effects of loading

The first step to determine the final deflection is to consider a Navier's solution for deflection at any point of the plate:

$$v_q(x,y) = \frac{16 \cdot q}{D \cdot \pi^6} \cdot \sum_{m=1}^{\infty} \sum_{n=1}^{\infty} \frac{\sin \frac{m \cdot \pi \cdot x}{a} \cdot \sin \frac{n \cdot \pi \cdot y}{b}}{m \cdot n \cdot \left[\left(\frac{m}{a}\right)^2 + \left(\frac{n}{b}\right)^2 \right]}$$

With q is the uniform applied distributed load, D the bending stiffness, E the Young's modulus, t the cassette thickness and ν the Poisson's ratio:

$$D = \frac{E \cdot t^3}{12 \cdot (1 - \nu^2)}$$

The rotational stiffness of edges is taken into account across a coefficient from beam theory:

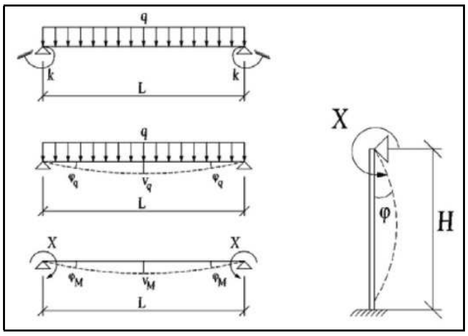

Figure 15: Models used for beam theory

And the maximum deflection to the centre of the plate is determined by:

$$v_m = v_m \cdot \left[1 - \frac{4}{5 \cdot \left(\frac{H}{2 \cdot L} + 1 \right)} \right]$$

In addition, maximum stresses at mid-point of the plate are determined:

$$\sigma_x = \frac{6}{t^3} \cdot M_x$$

$$\sigma_y = \frac{6}{t^3} \cdot M_y$$

2.1.3. Resistance of the cladding cassette [4]

Resistance of the cladding cassette is determined considering the edge as showed below:

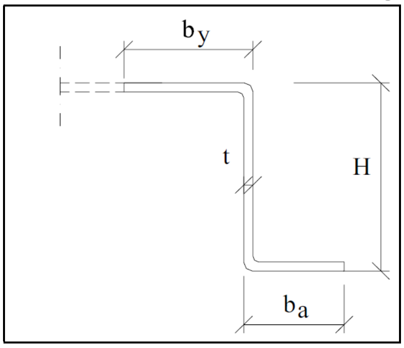

Figure 16: Edge of the cladding cassette

Under wind pressure, the top flange b_y is compressed and under wind suction is b_a.

To determine the effective part of b_a and b_y of this simulated simple supported beam, the outstanding element buckling value k_σ and the gross cross section is used with assume $k_\sigma = 0{,}43$:

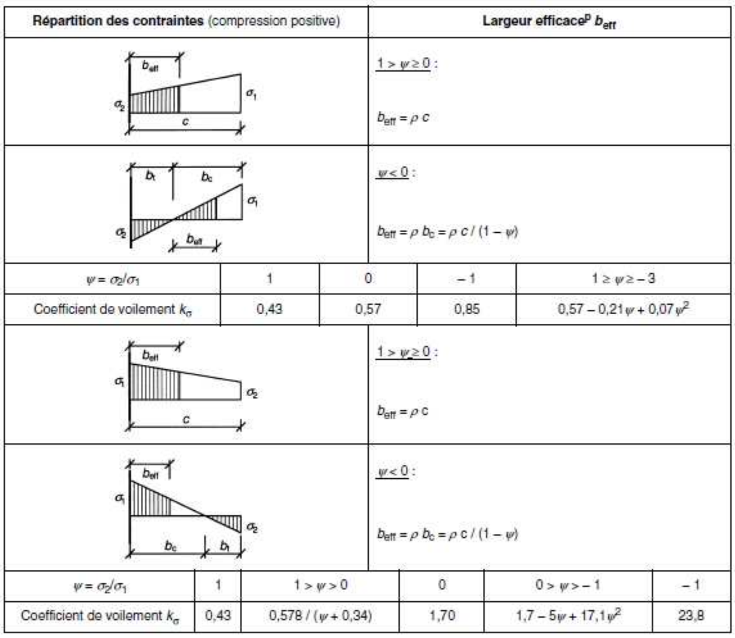

Répartition des contraintes (compression positive)	Largeur efficace^p b_{eff}
	$1 > \psi \geq 0$: $b_{eff} = \rho\, c$
	$\psi < 0$: $b_{eff} = \rho\, b_c = \rho\, c\,/\,(1-\psi)$

$\psi = \sigma_2/\sigma_1$	1	0	−1	$1 \geq \psi \geq -3$
Coefficient de voilement k_σ	0,43	0,57	0,85	$0{,}57 - 0{,}21\psi + 0{,}07\psi^2$

	$1 > \psi \geq 0$: $b_{eff} = \rho\, c$
	$\psi < 0$: $b_{eff} = \rho\, b_c = \rho\, c\,/\,(1-\psi)$

$\psi = \sigma_2/\sigma_1$	1	$1 > \psi > 0$	0	$0 > \psi > -1$	−1
Coefficient de voilement k_σ	0,43	$0{,}578\,/\,(\psi + 0{,}34)$	1,70	$1{,}7 - 5\psi + 17{,}1\psi^2$	23,8

Figure 17: Buckling coefficient defined in EN 1993–1–3

The effective widths b_{eff} are the minimum between effective b_a and effective by; and the new cross section presents both flanges fully effective:

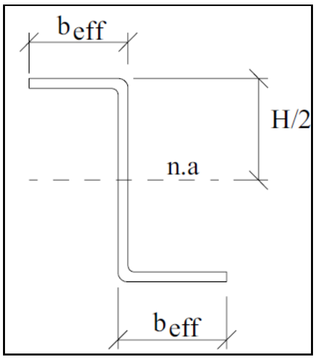

Figure 18: Section with two b_{eff} wide flanges

To determine the effective part of b_a and by, the reduction factor ρ, from ENV 1993-1-3, is used as following:

If $\bar{\lambda}_p \leq 0.673$: $\rho = 1.0$

If $\bar{\lambda}_p > 0.673$: $\rho = (1.0 - \frac{0.22}{\bar{\lambda}_p})/\bar{\lambda}_p$, where:

$$\bar{\lambda}_p = \sqrt{\frac{f_y}{\sigma_{cr}}} \equiv \frac{b_p}{t}\sqrt{\frac{12(1-v^2)f_y}{\pi^2 E k_\sigma}}$$

, where: b_p is the nominal width of the plate element under consideration and f_y is the yield stress (or, more precisely, 0.2% proof strength) for the copper sheet.

Figure 19: Reduction factor ρ

The effective parts of the web are calculated with $k_\sigma = 4$ like paragraph 1.2.2.2 above. The final effective section of the cassette edge is yet represented following:

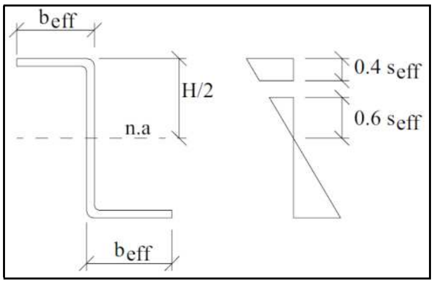

Figure 20: Effective section

The last step consists to determine the effective bending modulus W_{eff} and consequently the bending resistant moment:

$$M_{c,Rd} \leq W_{eff} \cdot \frac{f_y}{\gamma_{M1}}$$

2.1.4. Resistance of the screws at Ultimate Limit States

This design is made following the recommendations of ENV 1993-1-3. Dimensional criteria must be satisfied:

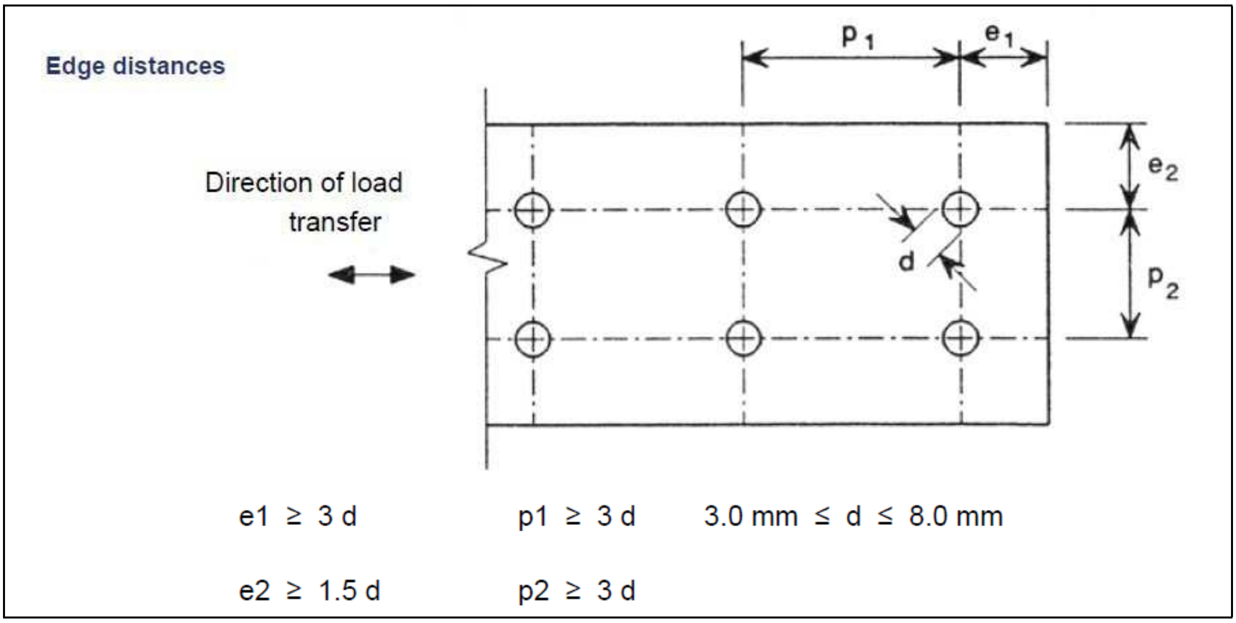

Figure 21: Edge and screw distances

Three kind of verification are established:

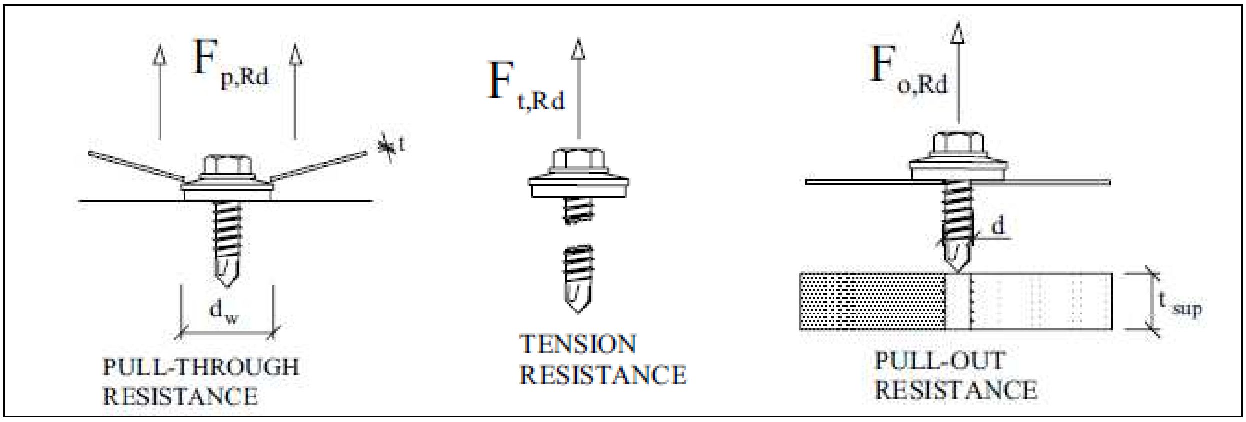

Figure 22: Type of fracture for screw

Using the following formulas:
For pull-through resistance:

$$F_{p,Rd} = 0,5 \cdot d_w \cdot t \cdot \frac{f_u}{\gamma_{M2}}$$

For pull-out resistance:

$$F_{o,Rd} = 0,65 \cdot d \cdot t_{\text{sup}} \cdot \frac{f_{u,\text{sup}}}{\gamma_{M2}}$$

Tension resistance, $F_{t,Rd}$ is given by the screw manufacturer (technical data by testing). With two conditions:

- $F_{t,Rd} \geq F_{p,Rd}$
- $F_{t,Rd} \geq F_{o,Rd}$

2.2. Analysis of the method showed

Method used to determine loading effects is limited to cassette on 4 simply supports, and this type of configuration not include cassettes on 2 simply supports and 2 others free.
Using Navier's solution is correct for plate on 4 supports. In this case, the deflection at the centre is:

$$v_q = \frac{5 \cdot q \cdot a^2 \cdot b^2}{384 \cdot D} \cdot f(\rho)$$

With:

$$\rho = a/b$$

The consequence of different boundary conditions could be appreciated using various models, for 2 simply supports and 2 free edges; Levy's model is one solution. In Reference [11] for square plate of a dimension, the author give for 4 simply supports a maximum displacement to the plate centre of (chapter II – paragraph 7):

$$v_q = 0,318 \cdot \frac{15 \cdot q \cdot a^4}{4 \cdot E \cdot I \cdot \pi^5}$$

Using Navier's solution, while Levy's solution gives for 2 simply supports combined with 2 free edges (chapter V – paragraph 15):

$$v_q = 0,994 \cdot \frac{15 \cdot q \cdot a^4}{4 \cdot E \cdot I \cdot \pi^5}$$

In addition, the method described here for calculating deflection not takes account of edges behaviour (and edges effective inertia). It could be appear secure but the obtained result is a deflection between the centre of the plate and these edges.

Concerning the determination of the resistance of the cassette, the references of the formulas aren't updated:

- Buckling coefficient k_σ into EN 1993-1-5,
- Reduction factor ρ into EN 1993-1-5,
- Relation to determine $\bar{\lambda}_p$ incorrect,
- New criteria for pull-out resistance for screw (depending of the thread).

2.3. Interest and conclusion about the method for WP4

The method is simple and use general knowledge of plate theory combined to Eurocode formulas.
Boundaries conditions must be taken into account in order to choose the correct model for the deflection using for example Levy's model or more recent solution.
Eurocodes reference formulas must be updated.
This method, after updating, should be a good estimation for behaviour of cladding cassette but not for cladding planks due to the specificity of the hidden longitudinal joint.

3. Conclusion and problematic of cladding planks with hidden longitudinal joints

The method described in paragraphs 1.2.2 and 2.1.3, after updating, should be a good estimation for behaviour of cladding cassette but not for cladding planks due to the specificity of the hidden longitudinal joint.
As we showed in paragraph 1.2.1, its design under wind suction is based on test and the main difficulty for WP4 will be to determine the behaviour of the longitudinal hidden joint between two planks (cf. Figure 1).

References

[1] DIN 18807-1, Trapezoidal sheeting in building; trapezoidal steel sheeting: general requirements and determination of loadbearing capacity by calculation

[2] DIN 18807-2, Trapezoidal sheeting in building; trapezoidal steel sheeting: determination of loadbearing capacity by testing.

[3] NF P 34-503, Profiled sheeting made of coated or non-coated steel sheet and panels – Bending tests under linear loads and/or under concentrated loads.

[4] EN 1993-1-3, Eurocode 3 – Design of steel structures – Part. 1-3: General rules – Supplementary rules for cold-formed members and sheeting.

[5] EN 1993-1-5, Design of steel structures – Part 1-5: Plated structural elements.

[6] ETAG 034, Guideline for European Technical Approval of kits for external wall claddings, Part I: Ventilated cladding kits comprising cladding components and associated fixings.

[7] ETAG 034, Guideline for European Technical Approval of kits for external wall claddings, Part II: Cladding kits comprising cladding components, associated fixings, subframe and possible insulation layer.

[8] Book CSTB 3517, Methods for testing resistance to wind load on cladding systems, claddings.

[9] LUVATA, Nordic systems copper – Facade, roof and rainwater structures.

[10] Book CSTB 1564, DTU P22-703, Design rules constructions with thin wall elements – Justification by designing the safety of buildings.

[11] E. ESTANAVE: Contribution to the study of elastic equilibrium of rectangular thin plate, Scientific Annals of E.N.S. 3th serial, tome 17 (1900) pp. 295-358.